Ion channels of *Fasciola hepatica* incorporated into planar lipid bilayers

J. H. JANG[1], S. D. KIM[1], J. B. PARK[2], S. J. HONG[3] *and* P. D. RYU[1]*

[1] *Laboratory of Pharmacology, College of Veterinary Medicine and School of Agricultural Biotechnology,*
Seoul National University, San 56-1 Sillim-dong, Kwanak-gu, Seoul 151-742, Republic of Korea
[2] *Department of Physiology, Chungnam National University College of Medicine, Taejeon 130-131, Republic of Korea*
[3] *Department of Parasitology, Chung-Ang University College of Medicine, Seoul 156-756, Republic of Korea*

SUMMARY

Ion channels are important target sites of anthelmintics, but little is known about those in *Fasciola hepatica*. In this work, we applied a planar lipid bilayer technique to characterize the properties of single ion channels in *F. hepatica*. Under a 200/40 mM KCl gradient, a large conductance channel of 251 pS was observed in 18% of the membranes studied. The channel was selective to K^+ over Cl^- with a permeability ratio of K^+ to Cl^- (P_K/P_{Cl}) of 4·9. Open state probability (P_o) of the channel was less than 0·5 and dependent on voltage ($-60 \sim +40$ mV) and Ca^{2+} ($\sim 100\,\mu$M). The other two types of single channels observed in 11 and 5% of membranes, respectively, were a K^+-permeable channel of 80 pS ($P_K/P_{Cl}=4·6$) and a Cl^--permeable channel of 64 pS ($P_K/P_{Cl}=0·058$). Open state probability of both channels showed little voltage dependence. The results indicate that distinct single channels of $60 \sim 251$ pS are present in relative abundance and, in addition, that the planar lipid bilayer technique can be a useful tool for the study of single ion channels in *F. hepatica*.

Key words: ion channels, *Fasciola hepatica*, planar lipid bilayer.

INTRODUCTION

Voltage- and ligand-gated ion channels are an important family of membrane proteins involved in the neuromuscular physiology of flatworms such as *Schistosoma mansoni* and *Fasciola hepatica* (Pax *et al.* 1996). Several clinically useful anthelmintic drugs are known to act on *ligand-gated ion* channels such as nicotinic acetylcholine receptor channels, GABA-gated chloride channels and glutamate-gated chloride channels (Martin, 1997; Martin, Robertson & Bjon, 1997). Numerous studies have characterized the ion channels in *S. mansoni*, including Ca^{2+} channels (Kohn *et al.* 2001*a,b*), K^+ channels (Blair *et al.* 1991; Day, Bennett & Pax, 1992; Kim *et al.* 1995), non-selective cation channels (Day *et al.* 1992) and ryanodine receptor channels (Silva *et al.* 1998; Day *et al.* 2000). In *F. hepatica*, a major flatworm causing productivity loss in domestic animals (Loyacano *et al.* 2002) as well as fasciolosis in humans (Chen & Mott, 1990; Mas-Coma, Esteban & Barques, 1999), a hyperpolarization-activated cation current was recently identified in acutely isolated single cells by whole-cell patch-clamp technique (Kim *et al.* 2002). However, the properties of various ion channels in *F. hepatica* remain largely unknown.

Currently, the patch clamp technique is widely used for the study of ion channels and currents in a variety of tissues. For the ion channels of flatworms, it is known that the irregular surface of the worm limited the efficiency of the patch clamp study (Day *et al.* 1992). To access ion channels present in such an irregular structure, a vesicle preparation from the tegument of *S. mansoni* (Robertson, Martin & Kusel, 1997) and whole worm microsomes of *Echinococcus granulosus* (Grosman & Reisin, 1995, 1997) have been used for patch clamp and planar lipid bilayer recordings, respectively. In this work, we present the basic properties of 3 types of ion channels in *F. hepatica* incorporated into planar lipid bilayers.

MATERIALS AND METHODS

Fasciola hepatica

Metacercariae of *F. hepatica* were purchased from Baldwin Aquatics (Monmouth, OR, USA). Male rats (Sprague-Dawley) were inoculated with metacercaria (5–20/rat). After 12 weeks (Sukhdeo, Sukhdeo & Mattrick, 1988), mature *F. hepatica* were recovered from the bile duct of infected rats, stored at $-70\,^\circ$C in saline, and used for preparing vesicles.

Vesicle preparations

Vesicles of *F. hepatica* were made by a modified method of Guo *et al.* (1987). Approximately 15–20 g of *F. hepatica* were suspended in 3 volumes of

* Corresponding author: Laboratory of Pharmacology, College of Veterinary Medicine, Seoul National University, San 56-1 Sillim-dong Kwanak-gu, Seoul 151-742, Republic of Korea. Tel: +82 2 880 1254. Fax: +82 2 879 0378. E-mail: pandryu@plaza.snu.ac.kr

sucrose buffer. The sucrose buffer contained 0·3 M sucrose, 10 mM HEPES, 0·2 mM EDTA, and 3 mM NaN₃, and the pH was adjusted to 7·4 with 2 M NaOH. The worms were minced with surgical scissors and centrifuged at 100 *g* for 5 min. The resulting pellets were resuspended in 0·3 M sucrose buffer containing protease inhibitors, phenylmethylsulfonylfluoride (0·3 mM) and leupeptin (0·5 μg/ml), and then homogenized with a polytron homogenizer (Brinkmann Instrument Inc, Switzerland). The homogenate was centrifuged at 1500 *g* for 15 min and the supernatant was centrifuged at 10 000 *g* for 15 min. Granules of KCl were added to the resulting supernatant to 0·6 M and allowed to stand on ice for 30 min. The microsomes were pelleted at 100 000 *g* (SW41TI rotor, optima XL-100K ultracentrifuge, Beckman, USA) for 1 h. The resulting pellets were dissolved using a syringe needle (26 gauge) and resuspended in 0·3 M sucrose buffer in a final volume of 4–5 ml. This suspension was layered over a discontinuous step-gradient of sucrose (20, 30 and 40%). The samples were centrifuged at 130 000 *g* (SW41TI rotor) for 3 h, and the microsomal fractions banding at the 10/20%, 20/30% and 30/40% interfaces were separately collected with a Pasteur pipette. Each fraction was diluted with a double amount of distilled water and centrifuged at 100 000 *g* for 1 h. All steps were carried out either on ice or at 2 °C to minimize protein degradation. The resulting pellets were divided into small aliquots (20–30 μl) and stored at −70 °C until use.

Planar lipid bilayers and vesicle fusion

PE (1-palmitoyl-2-oleoyl-sn-Glycero-3-phosphoethanolamine), PC (1-palmitoyl-2-oleoyl-sn-Glycero-3-phosphocholine), and PS (1-palmitoyl-2-oleoyl-sn-Glycero-3-phosphoserine) were purchased from Avanti Polar Lipids (Alabaster, AL, USA). Lipid stock solutions were kept in chloroform and stored at −70 °C. Lipid working solution was prepared daily at 25 mg/ml in decane (PE : PC : PS = 70 : 20 : 10) unless otherwise described. The recording chamber is composed of 2 compartments: a polystyrene cup (*trans* compartment) and a rectangular chamber (*cis* compartment). The *trans* and *cis* compartments were filled with 0·6 and 1·2 ml aqueous solutions containing 40 mM KCl, 10 mM N-[2-hydroxyethyl]-piperazine-N′-[2-ethanesulfonic acid] (HEPES) and pH 7·4 which was adjusted with 1 M N-methyl D-glucamine (NMDG). A planar bilayer was formed between the 2 compartments by painting the lipid solution with a thin glass rod over an aperture (diameter, 200 μm) of the polystyrene cup. Formation of the bilayer was visualized on an oscilloscope screen as an increase of membrane capacitance, while applying a triangular voltage wave under voltage clamp. When the capacitance of the membranes increased to 100–200 pF, the concentration
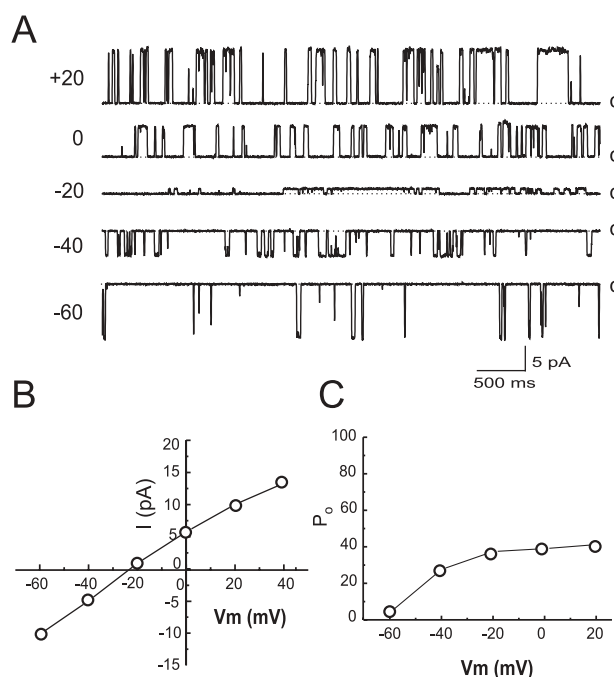

Fig. 1. Single channel currents of the large conductance K⁺-permeable channel from *Fasciola hepatica*.
(A) Current traces recorded under 200/40 (*cis/trans*) mM KCl gradient. Numbers at the left of each trace indicate transmembrane voltage and 'c's at the right indicate closed states. (B and C) Current–voltage relations (B) and voltage dependence of open state probability (C) of the channel shown in (A). Slope conductance = 239 pS.

of KCl and CaCl₂ was adjusted to 200 mM and 30–100 μM, respectively, by adding the appropriate amount of stock solutions (3 M KCl and 100 mM CaCl₂) to the *cis* compartment. Then, a small amount (1–5 μl) of microsomes was added to the *cis* compartment and the *cis* compartment suspension was continuously stirred with a small magnetic stirring bar (1 × 3 mm) until fusion was detected.

Electrical measurements and data analysis

Currents were measured at constant voltage with a bilayer amplifier (BC525A, Warner Instr. Co., Hamden CT, USA). The current signal was defined as positive when it flowed from *cis* to *trans*. The junction potential between chamber and headstage of the amplifier was adjusted before the bilayers were formed. Electrical contacts were made through 2 Ag/AgCl electrodes. The sides of each electrode contacted were for voltage command and current measurement. The other sides of each electrode were suspended in 2 wells, filled with 0·5 M KCl. The 2 wells and *cis/trans* compartments were connected by an agar bridge. This agar bridge was a U-shaped microelectrode filled with boiled agar solution (3%) containing 0·2 M KCl, 1 mM EGTA. Single channel current data were filtered at 500 Hz by an 8-pole
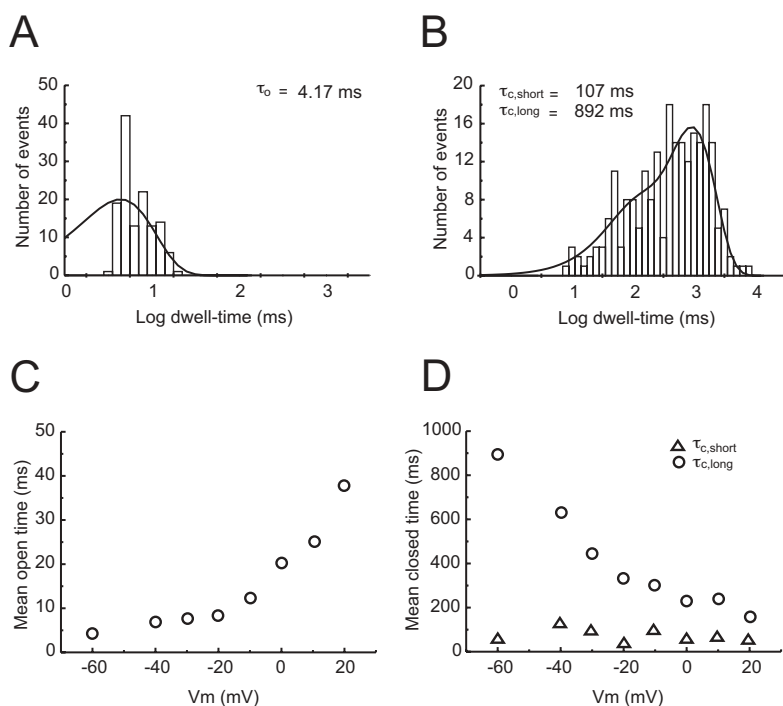
A

B

C

D

Fig. 2. Dwell time distribution of a large conductance K^+-permeable channel and its voltage dependence. (A and B) Open- (A) and closed- (B) dwell times were fitted with 1 and 2 exponentials, respectively. τ_o, mean open time; $\tau_{c,long}$ and $\tau_{c,short}$, mean closed times of short and long durations, respectively. Mean open time was 4·17 ms (event number = 131) and mean closed times were 107 and 892 ms (event number = 228), respectively. (C and D) Relations between voltage and mean dwell times of open (C) and closed (D) states. Single channel current was recorded under symmetrical 200 mM KCl. Filtered at 200 Hz and digitized at 2 kHz.
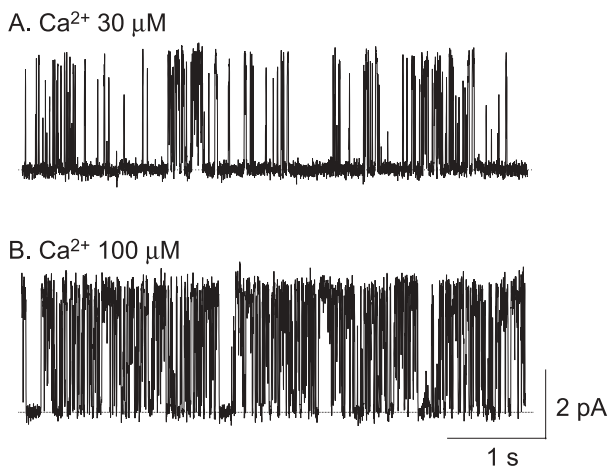
A. Ca^{2+} 30 µM

B. Ca^{2+} 100 µM

2 pA

1 s

Fig. 3. Single channel current of a large conductance K^+-permeable channel recorded at 30 (A) and 100 µM Ca^{2+} (B). P_o, measured from the current record of 74 and 57 s, increased from 0·14 to 0·3 in response to elevation of Ca^{2+} concentration in the *cis* compartment. The current was recorded at +20 mV and symmetrical 200 mM KCl from a planar lipid bilayer (PE : PC = 80 : 20).

Bessel filter and digitized on a PC at 2 kHz using a Digidata 1200 data acquisition unit (Axon Instr. Co., Foster City, CA, USA). The analog data were also stored on VTR tapes using a VR-10B digital data recorder (Instrutech. Corp., New York, NY, USA) and recorded on a pen recorder. Parameters analysed were current amplitude, open state probability and mean dwell times. These parameters were measured by using the software for analysis of single channel current, pClamp (Ver 6.0, Axon Instr. Co., Foster City, CA, USA). The relative permeability of Cl^- to that of K^+ was calculated from the measured reversal potentials according to the following Goldman–Hodgkin–Katz Equation (Labarca & Latorre, 1992):

$$V_{rev} = RT/zF * \ln\{(P_K*[K]_{trans} + P_{Cl}*[Cl]_{cis})/ (P_K*[K]_{cis} + P_{Cl}*[Cl]_{trans})\}$$

where V_{rev}, P_K, P_{Cl}, $[K]_{trans}$ and $[Cl]_{cis}$ stand for measured reversal potential, permeability of K^+ and Cl^- ions, and concentrations of *trans* K^+ and *cis* Cl^- ions, respectively. R, T, F and z are the gas constant, absolute temperature, Faraday constant and ionic valence, respectively.

Experimental data were expressed as mean ± S.E.M. (standard error of mean) and the number of membranes tested and analysed was represented by '*n*'. The statistical significance of data was determined using independent Student's *t*-test for the comparison of two means and a level of $P < 0·05$ was considered to be significant.
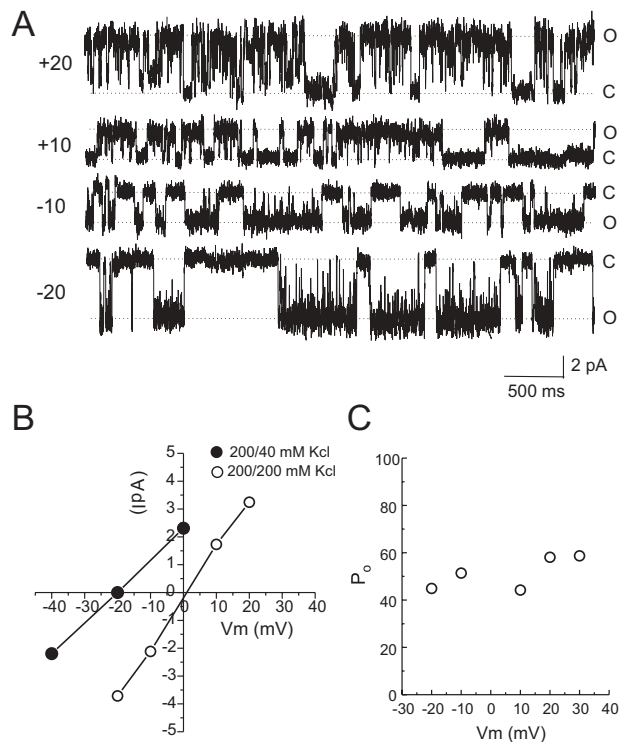
Fig. 4. Single channel activity of a small conductance K^+-permeable channel. (A) Representative current traces recorded at various voltages. (B) Current–voltage relations of the small conductance K^+-permeable channel shown in (A) under unsymmetrical (200/40 mM) and symmetrical (200/200 mM) KCl gradients. Respective slope conductances were 112 and 177 pS. (C) Open state probability at various membrane potentials.

RESULTS

Based on the amplitude and the direction of current flow at 0 mV and 200/40 (*cis/trans*) mM KCl gradient, we identified 3 types of ion channels of *F. hepatica* incorporated into the planar lipid bilayer. They were a large and a small K^+-permeable channel, and a Cl^--permeable channel. Among the total of 188 bilayers that showed single channel activity, the large K^+-permeable channel ($250 \cdot 5 \pm 5 \cdot 9$ pS, mean $\pm$ S.E.M.; range, 194–309 pS; $n = 33$) was most frequently recorded (17·5%). The small K^+-permeable ($79 \cdot 6 \pm 4 \cdot 4$ pS; range, 55–112 pS; $n = 21$) and the Cl^--permeable ($63 \cdot 9 \pm 5 \cdot 9$ pS; range, 42–97 pS; $n = 10$) channels were recorded from 11·2 and 5·3% of the bilayers, respectively. The rest of the bilayers showed currents of multi-channels or leakage (35·7%), and these were not further analysed. Most ion channels presented in this work were obtained from the microsomes banded in the 20/30% sucrose interface.

Large conductance K^+-permeable channel

Fig. 1 illustrates the single channel property of a large conductance K^+-permeable channel from *F. hepatica*. Representative single channel traces show

a discrete gating activity of ~ 5 pA under a condition of 0 mV, 200/40 (*cis/trans*) mM KCl gradient and 100 μM $[Ca]_{cis}$ (Fig. 1A). The current-voltage relations were linear (Fig. 1B) and the mean slope conductance of 5 channels was 227 ± 38 pS. The reversal potential was $-22 \cdot 6 + 1 \cdot 9$ mV ($n = 5$) and the ratio of permeability of K^+ to that of Cl^- (P_K/P_{Cl}) was $4 \cdot 86 \pm 0 \cdot 75$. In a typical channel, open state probability (P_o) of the channel was higher when the *cis* side was positive and lower when it was negative (Fig. 1C), but overall P_o remained less than 0·5 over the voltage range of -60 to $+20$ mV. Dwell times of open and closed states were fitted with 1 and 2 exponentials and their mean times were 4·2 ms (τ_o) for open states, and 107 ($\tau_{c,short}$) and 892 ms ($\tau_{c,long}$) for closed states. When the voltage was increased towards positive, τ_o increased, but $\tau_{c,long}$ decreased (Fig. 2C and D). P_o of the channel increased with increasing Ca^{2+} in the *cis* compartment from 30 to 100 μM (Fig. 3).

Small conductance K^+-permeable channel

Fig. 4 illustrates the single channel property of a typical small conductance K^+-permeable channel. The current traces shown in Fig. 4A illustrate that open dwell times were better resolved than those of large conductance K^+-permeable channels. Its current–voltage relations were linear with slope conductance of $79 \cdot 6 \pm 4 \cdot 4$ pS ($n = 21$) under the unsymmetrical 200/40 (*trans/cis*) mM. The reversal potential was $-23 \cdot 4 \pm 1 \cdot 3$ mV ($n = 4$) and the resulting P_K/P_{Cl} was $4 \cdot 6 \pm 0 \cdot 5$ (Fig. 4B). The conductance of the small K^+-permeable channel was significantly smaller than that of the large K^+-permeable channels ($P < 0 \cdot 0005$), but the reversal potentials of both channels were not significantly different ($P > 0 \cdot 25$), indicating that both are selective for K^+ over Cl^-. P_o did not show remarkable voltage dependence and remained at about 0·5 over the voltage range of $-20-+30$ mV. The overall increase in P_o was 0·028/10 mV over the voltage range of -20 to 30 mV (Fig. 4C). Dwell time histograms of the currents of the same channel indicated that mean open times were well described by 1 exponential ($\tau_o = 31 \cdot 3$ ms), but that mean closed times were fitted with 2 exponentials: $\tau_{c,short} = 8 \cdot 0$ (86%), $\tau_{c,long} = 63 \cdot 3$ (13%) ms (Fig. 5A and B). In contrast to P_o, the mean times of both open and closed states, decreased with the increase of membrane voltage (Fig. 5C and D). In this channel, the frequency of channel openings was 5·1, 6·9, 6·4, 9·8, and 13·5 Hz at -20, -10, 10, 20, and 30 mV, respectively, suggesting a voltage-dependent increase in gating activity with little change in P_o.

Cl^--permeable channel

The currents of the Cl^--permeable channels were readily distinguished from those of the K^+-permeable channels by the downward shift at open
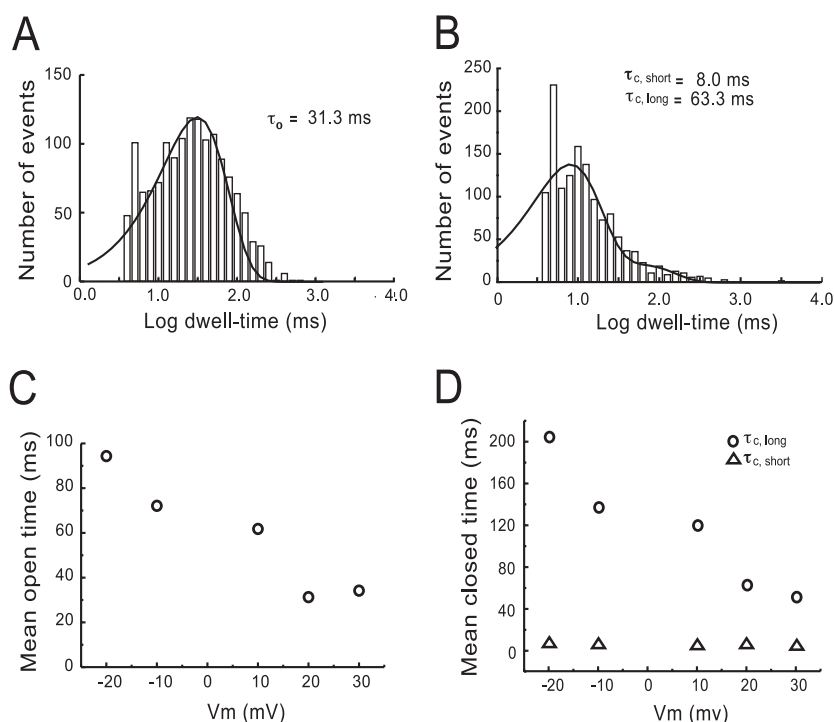
Fig. 5. Dwell time distribution of a small conductance K^+-permeable channel and its voltage dependence. (A and B) Open- (A) and closed- (B) dwell times were fitted with 1 and double exponentials, respectively. τ_o, mean open time; $\tau_{c,long}$ and $\tau_{c,short}$, mean closed times of short and long durations. Mean open time was 31·3 ms (event number = 1451) and mean closed times were 8·0 and 63·3 ms (event number = 1355). (C and D) Mean dwell times of open (C) and closed (D) states were measured at +20 mV and symmetrical conditions.
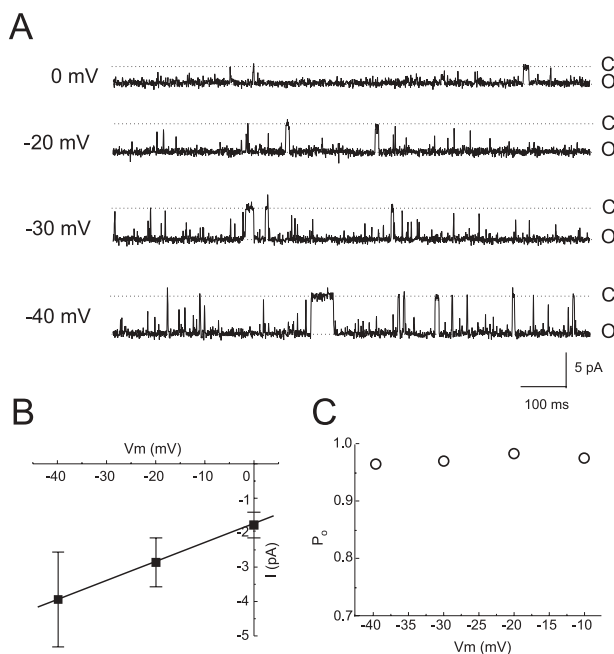

Fig. 6. Single channel currents of the Cl^--permeable channel from *Fasciola hepatica*. (A) Representative traces of a Cl^--permeable channel under 200/40 mM KCl gradient. (B) Averaged current–voltage relations of the Cl^--permeable channels at various membrane potentials. (C) Open state probability of the Cl^--permeable channel shown in (A).

states. The representative traces of a Cl^--permeable channel show long open dwell times typical to this type of channel (Fig. 6A). The current-voltage relation of the Cl^--permeable channel current was linear and the mean slope conductance from 6 channels was $52·3 \pm 8·0$ pS (Fig. 6B). The mean reversal potential in unsymmetrical conditions was $35·8 \pm 3·5$ mV and the resulting P_K/P_{Cl} was $0·058 \pm 0·03$. P_o of the channel remained close to unity and showed little voltage dependence over the voltage range tested (Fig. 6C). Analysis of dwell time histograms of single-channel recording at -30 mV revealed that mean open times were described by one exponential ($\tau_o = 201$ ms), but that mean closed times were described by 2 exponentials ($\tau_{c,short} = 1·6$ ms, $\tau_{c,long} = 13·7$ ms; Fig. 7A and B). Although the apparent P_o showed negligible voltage dependence (Fig. 6C), τ_o increased when the voltage increased towards positive, but $\tau_{c,long}$ decreased, indicating the voltage dependence in the gating of the Cl^--permeable channel (Fig. 7C and D).

DISCUSSION

In this study, we characterized 3 types of single ion channels from *F. hepatica* incorporated into planar lipid bilayers: a large and a small conductance K^+-permeable channel, and a Cl^--permeable channel. The 2 K^+-permeable channels were similar in ion selectivity (P_K/P_{Cl}, 4·9 *vs* 4·6, $P > 0·25$), but different in their conductance (251 *vs* 80 pS, $P < 0·0005$)
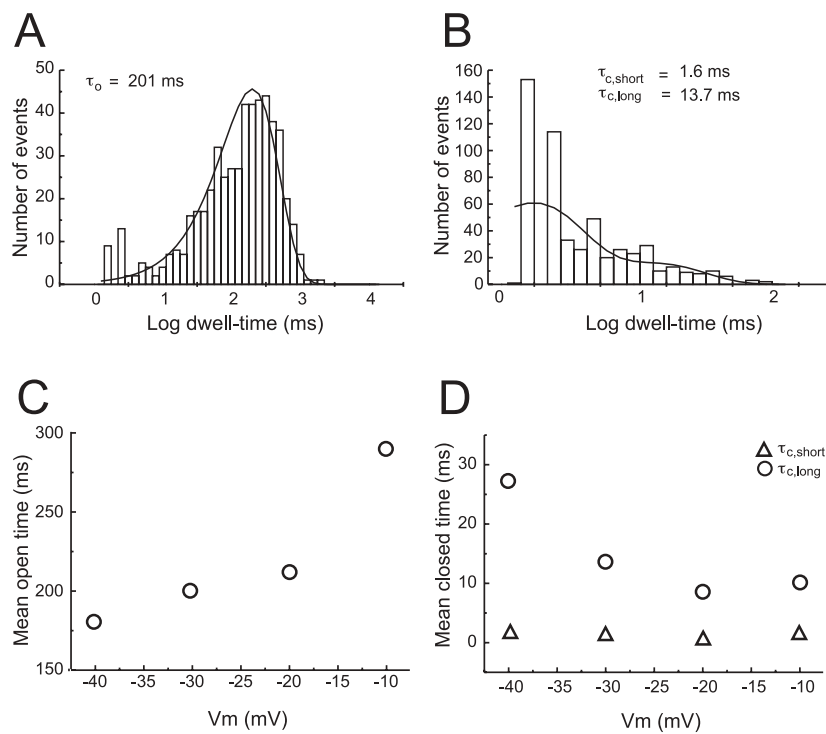
Fig. 7. Dwell time distribution of a Cl^--permeable channel and its voltage dependence. (A and B) Histograms of open- (A) and closed- (B) states at -30 mV. Dwell times of opening and closing were fitted with 1 (τ_o) and 2 exponentials ($\tau_{c,long}$ and $\tau_{c,short}$), respectively, by the maximum likelihood fitting method. (C and D) Mean open- (C) and closed- (D) dwell times at various voltages.

and voltage-dependence of P_o and τ_o. The activity of the large-conductance K^+-permeable channel was increased by Ca^{2+} in the *cis* compartment. The Cl^--permeable channel was readily distinguished from the K^+-permeable channels because of its high anion selectivity (P_K/P_{Cl}, 0·058), large τ_o (>175 ms) and high P_o (~1). The results will broaden our limited understanding on the ion channels present in *F. hepatica*.

The first type of ion channel of *F. hepatica*, the large conductance K^+-permeable channel, was recognized by its large conductance, 251 pS at 200/40 mM KCl gradient. Such large conductance was also observed in non-selective cation channels in the tegument of *S. mansoni* (Day *et al.* 1992; Robertson *et al.* 1997), Ca^{2+}-activated K^+ channels in the isolated muscle cells of *S. mansoni* (Blair *et al.* 1991) and Ca^{2+}-dependent cation channel in *Echinococcus* (*E.*) *granulosus* (Grosman & Reisin, 1995). The conductances of these channels ranges between 195 and 360 pS at 144–200 mM symmetrical or unsymmetrical K gradients. Currently it is not certain whether the large conductance K^+-permeable channels of *F. hepatica* can pass cations other than K^+, but the other single channel properties of the large conductance K^+-permeable channels of *F. hepatica* are different from those of large conductance channels reported in *S. mansoni* and *E. granulosus*. For example, the large conductance non-selective cation channel in *S. mansoni* (Day *et al.* 1992; Robertson *et al.* 1997) has

high P_o and long open dwell times (~min), while the channel in *F. hepatica* has lower P_o and shorter open dwell times (~s). In addition, the subconductance state (~100 pS) present in the channel of *S. mansoni* was not observed from the channel of *F. hepatica*. The large conductance channel in *F. hepatica* is partially similar to the channel in *E. granulosus* (Grosman & Reisin, 1995); both channels are activated by Ca^{2+}, but the activity of the former was voltage-dependent, whereas that of the latter was not.

When compared with the Ca^{2+}-dependent K^+ channel of *S. mansoni* (Blair *et al.* 1991), the large conductance channels in *F. hepatica* and *S. mansoni* are similar in their large conductance, Ca^{2+}-dependence and high selectivity to K^+ over Cl^-. Therefore, it is likely that the large conductance K^+-permeable channel in *F. hepatica* is a member of the large-conductance Ca^{2+}-activated K^+ or 'BK' channel found in various animal species (Latorre *et al.* 1989). However, other critical properties such as the sensitivity to Ca^{2+} and ion selectivity to various cations should be further determined for the large conductance Ca^{2+}-activated K^+-permeable channels of *F. hepatica*.

The second type of single channel identified in *F. hepatica*, a small conductance K^+-permeable channel of 80 pS, is comparable to the non-selective cation channel recorded from the outer tegmental membrane of adult female *S. mansoni* in terms of its substate conductance (~100 pS) and selectivity to

cations (Day *et al.* 1992; Robertson *et al.* 1997). However, the channels of *S. mansoni* and *F. hepatica* are different in other aspects. The channel in *F. hepatica* showed discrete gating activity at various voltages with negligible voltage dependence in P_o, whereas the channel in *S. mansoni* showed little gating activity at a steady potential with higher P_o at negative potential (Day *et al.* 1992). Therefore, it is unlikely that the two types of single channel represent the same type of ion channels in these flatworms. The third type of single channel identified from *F. hepatica* is the Cl^--permeable channel of $63 \cdot 9 \pm 5 \cdot 9$ pS. From their larger conductance, it is apparent that the Cl^--permeable channels of this study are different from the Cl^- channel of 20 pS recorded from the tegumental membrane of adult male *S. mansoni* (Robertson *et al.* 1997).

In this work, we identified 3 types of single channels from *F. hepatica* using the planar lipid bilayer technique. The single channel properties of these channels and the recording method used can further help to understand the physiological and pharmacological significances of ion channels in *F. hepatica*.

REFERENCES

BLAIR, K. L., DAY, T. A., LEWIS, M. C., BENNETT, J. L. & PAX, R. A. (1991). Studies on muscle cells isolated from *Schistosoma mansoni*: a Ca^{2+}-dependent K^+ channel. *Parasitology* **102**, 251–258.

CHEN, M. G. & MOTT, K. E. (1990). Progress in assessment of morbidity due to *Fasciola hepatica* infection: a review of recent literature. *Tropical Disease Bulletin* **87**, R1–R38.

DAY, T. A., BENNETT, J. L. & PAX, R. A. (1992). *Schistosoma mansoni*: Patch-clamp study of a nonselective cation channel in the outer tegumental membrane of females. *Experimental Parasitology* **74**, 348–356.

DAY, T. A., HAITHCOCK, J., KIMBER, M. & MAULE, A. G. (2000). Functional ryanodine receptor channels in flatworm muscle fibres. *Parasitology* **120**, 417–422.

GROSMAN, C. & REISIN, I. L. (1995). *Echinococcus granulosus*: partial characterization of the conductive properties of two cation channels from protoscoleces of the ovine strain, reconstituted on planar lipid bilayers. *Experimental Parasitology* **81**, 546–555.

GROSMAN, C. & REISIN, I. L. (1997). Interconverting gating modes of a nonselective cation channel from the tapeworm *Echinococcus granulosus* reconstituted on planar lipid bilayers. *Journal of Membrane Biology* **158**, 87–94.

GUO, X., UEHARA, A., RAVINDRAN, A., BRYANT, S. H., HALL, S. & MOCZYDLOWSKI, E. (1987). Kinetic basis for

insensitivity to tetrodotoxin and saxitoxin in sodium channels of canine heart and denervated rat skeletal muscle. *Biochemistry* **26**, 7546–7556.

KIM, E., DAY, T. A., BENNET, J. L. & PAX, R. A. (1995). Cloning and functional expression of a Shaker-related voltage-gated potassium channel gene from *Schistosoma mansoni* (Trematoda: Digenea). *Parasitology* **110**, 171–180.

KIM, H. S., KAM, K. Y., RYU, P. D., HONG, S. J., JEON, J. S., JEON, B. H., KIM, K. J. & PARK, J. B. (2002). A gadolinium and PH-sensitive hyperpolarization-activated cation current in acutely isolated single neurons from *Fasciola hepatica*. *Parasitology* **125**, 423–430.

KOHN, A. B., LEA, J., ROBERTS-MISTERLY, J. M., ANDERSON, P. A. & GREENBERG, R. M. (2001*a*). Structure of three high voltage-activated calcium channel alpha1 subunits from *Schistosoma mansoni*. *Parasitology* **123**, 489–497.

KOHN, A. B., ANDERSON, P. A., ROBERTS-MISTERLY, J. M. & GREENBERG, R. M. (2001*b*). Schistosome calcium channel beta subunits. Unusual modulatory effects and potential role in the action of antischistosomal drug praziquantel. *Journal of Biological Chemistry* **276**, 36873–36876.

LABARCA, P. & LATORRE, R. (1992). Insertion of ion channels into planar lipid bilayers by vesicle fusion. *Methods in Enzymology* **207**, 447–463.

LATORRE, R., OBERHAUSER, A., LABARCA, P. & ALBAREZ, O. (1989). Varieties of calcium-activated potassium channels. *Annual Review of Physiology* **51**, 385–399.

LOYACANO, A. F., WILLIAMS, J. C., GURIE, J. & DEROSA, A. A. (2002). Effect of gastrointestinal nematode and liver fluke infections on weight gain and reproductive performance of beef heifers. *Veterinary Parasitology* **107**, 227–234.

MARTIN, R. J. (1997). Modes of action of anthelmintic drugs. *Veterinary Journal* **154**, 11–34.

MARTIN, R. J., ROBERTSON, A. P. & BJON, H. (1997). Target sites of anthelmintics. *Parasitology* **114**, S111–S124.

MAS-COMA, M. S., ESTEBAN, J. G. & BARQUES, M. D. (1999). Epidemiology of human fascioliasis: a review and proposed new classification. *Bulletin of the World Health Organization* **77**, 340–346.

PAX, R. A., DAY, T. A., MILLER, C. L. & BENNETT, J. L. (1996). Neuromuscular physiology and pharmacology of parasitic flatworms. *Parasitology* **113** (Suppl.), S83–S96.

ROBERTSON, A. P., MARTIN, R. J. & KUSEL, J. R. (1997). A vesicle preparation for resolving single-channel currents in tegument of male *Schistosoma mansoni*. *Parasitology* **115**, 183–192.

SILVA, C. L., CUNHA, V. M., MENDONCA-SILVA, D. L. & NOEL, F. (1998). Evidence for ryanodine receptors in *Schistosoma mansoni*. *Biochemical Pharmacology* **56**, 997–1003.

SUKHDEO, S. C., SUKHDEO, M. V. K. & METTRICK, D. F. (1988). Neurocytology of the cerebral ganglion of *Fasciola hepatica* (Platyhelminthes). *Journal of Comparative Neurology* **278**, 337–343.